Supporting Information

Thermally Stimulated Liquid Na–$CaCO_3$ Reaction: A Physico-Geometrical Kinetic Approach toward the Safety Assessment of Na-Cooled Fast Reactor

Nobuyoshi Koga[1,*] and Shin Kikuchi[2]

[1]Department of Science Education, Division of Educational Sciences, Graduate School of Humanities and Social Sciences, Hiroshima University, 1-1-1 Kagamiyama, Higashi-Hiroshima 739-8524, Japan
[2]Fast Reactor Cycle System Research and Development Center, Japan Atomic Energy Agency, 4002 Narita, Oarai, Higashi-Ibaraki 311-1393, Japan

Contents

* Corresponding Author, e-mail: nkoga@hiroshima-u.ac.jp

S1. Sample characterization

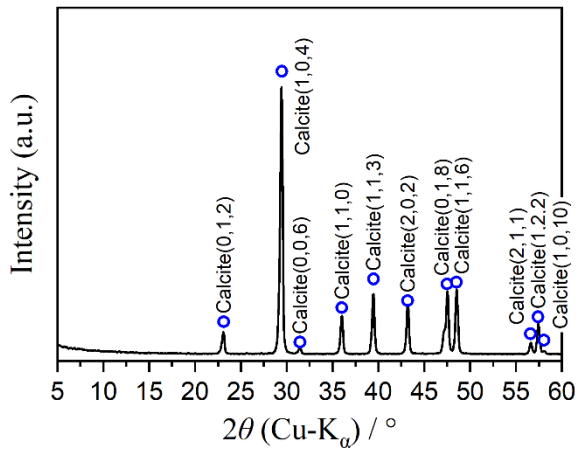

Figure S1. XRD pattern of the $CaCO_3$ sample.

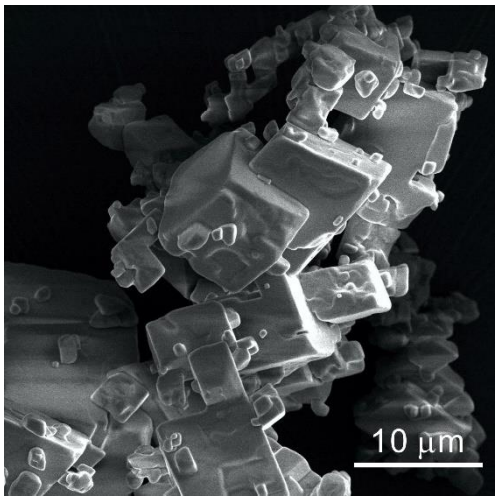

Figure S2. SEM images of the $CaCO_3$ sample particles.

S2. Liquid Na–$CaCO_3$ powder reaction

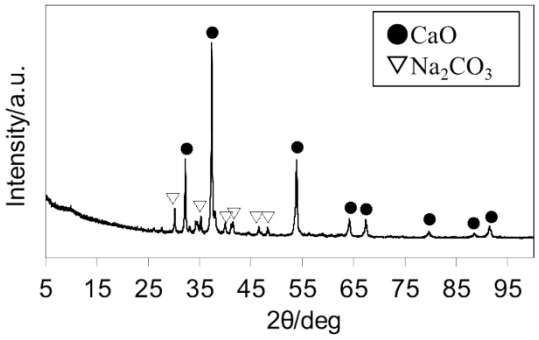

Figure S3. XRD pattern of the solid product recovered after the Na–$CaCO_3$ reaction

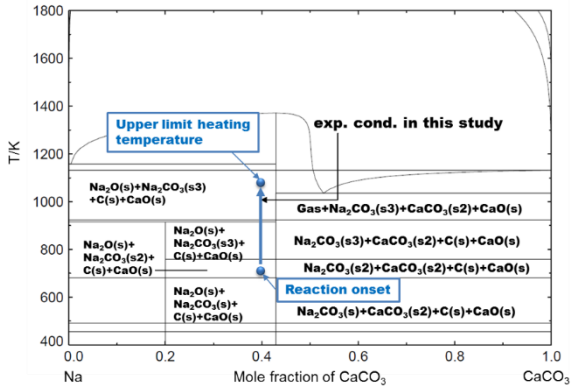

Figure S4. Phase diagram of the Na–$CaCO_3$ system drawn using a FactSage software [34].

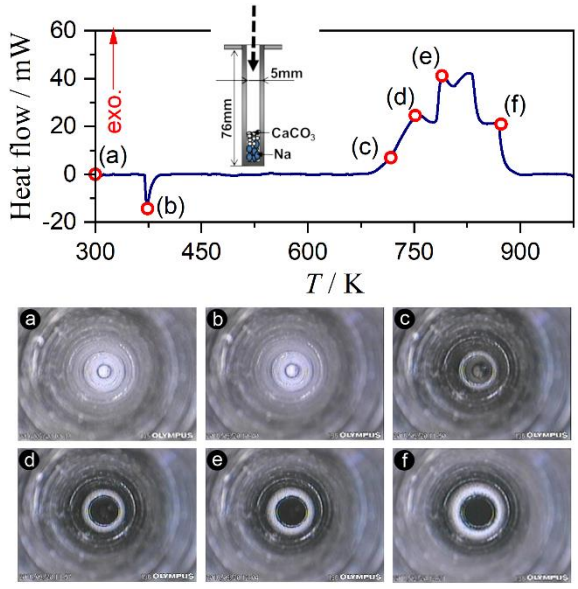

Figure S5. Change in the appearance of the top surface of the sample during the DSC measurements for the liquid Na–$CaCO_3$ powder reaction at a β of 5 K min^{-1}: (a) 300 K, (b) 374 K (the melting point of Na), **(c)** 717 K (the onset temperature of the liquid Na–$CaCO_3$ powder reaction), **(d)** 751 K (the first peak top), (e) 789 K (the second peak top), and (f) 873 K (the shoulder at the ending stage).

S3. Kinetics of the liquid Na–$CaCO_3$ powder reaction

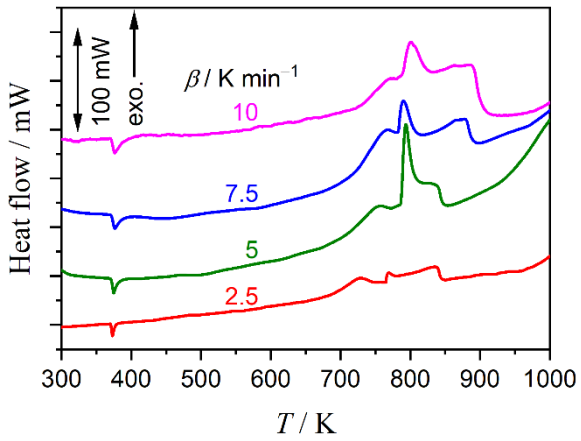

Figure S6. DSC curves for the Na–$CaCO_3$ powder (sampling conditions S1) at different β values.

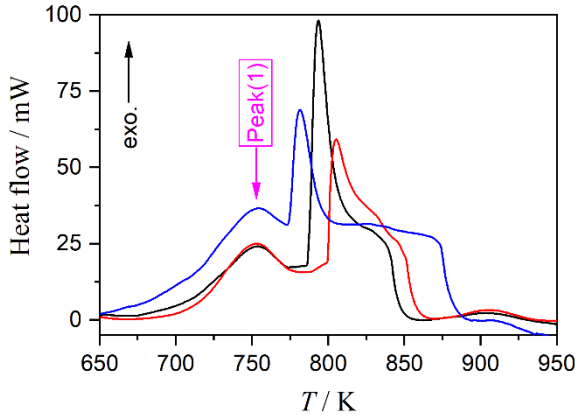

Figure S7. Repeatability of the DSC exothermic peaks for the liquid Na–$CaCO_3$ powder reaction recorded at a β of 5 K min^{-1}.

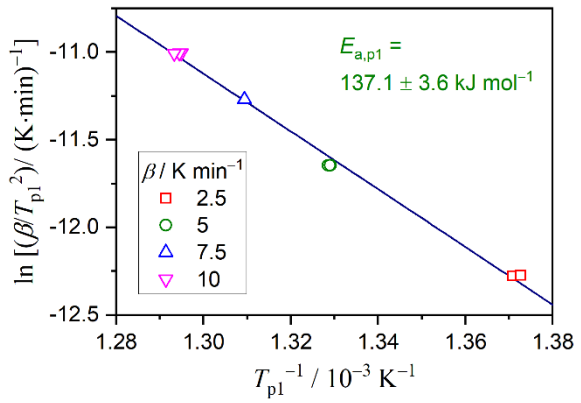

Figure S8. Kissinger plot for the first peak top of the exothermic DSC peaks attributed to the liquid Na–$CaCO_3$ powder reaction.

S4. Kinetics of the liquid Na–$CaCO_3$ pellet reaction

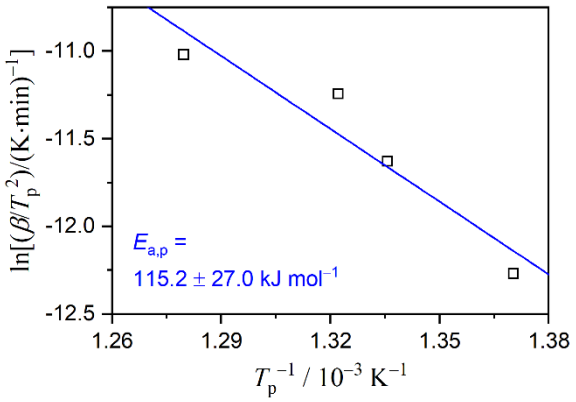

Figure S9. Kissinger plot for the peak top of the exothermic DSC peaks attributed to the liquid Na–$CaCO_3$ pellet reaction.

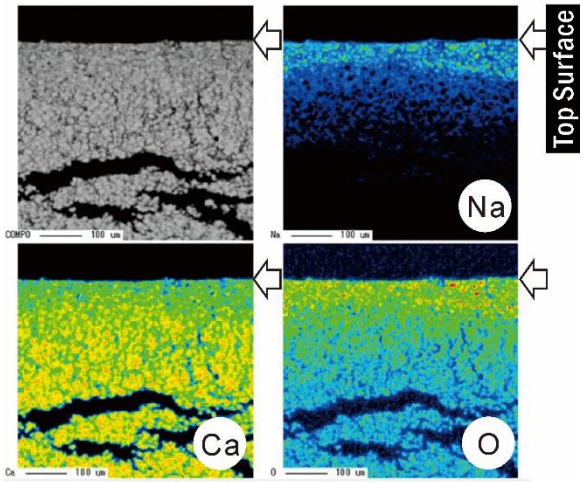

Figure S10. EPMA mapping of the cross section of the product of the liquid Na–$CaCO_3$ pellet reaction.

Mathematical deconvolution analysis

■ Pearson IV function

$$F(t) = \frac{a_0\left[1+\frac{\left(t-\frac{a_2a_4}{2a_3}-a_1\right)^2}{a_2^2}\right]^{-a_3}\exp\left[-a_4\left(\tan^{-1}\left(\frac{t-\frac{a_2a_4}{2a_3}-a_1}{a_2}\right)+\tan^{-1}\left(\frac{a_4}{2a_3}\right)\right)\right]}{\left(1+\frac{a_4^2}{4a_3^2}\right)^{-a_3}}, \quad \text{(S1)}$$

where a_0–a_4 indicate amplitude, center, width (>0), shape 1 (>0), and shape 2, respectively.

■ Asymmetric logistic function

$$F(t) = a_0\left[1+\exp\left(-\frac{t+a_2\ln a_3-a_1}{a_2}\right)\right]^{-a_3-1} a_3^{-a_3}(a_3+1)^{a_3+1}\exp\left(-\frac{t+a_2\ln a_3-a_1}{a_2}\right), \quad \text{(S2)}$$

where a_0–a_3 indicate amplitude, center, width (>0), and shape (>0), respectively.

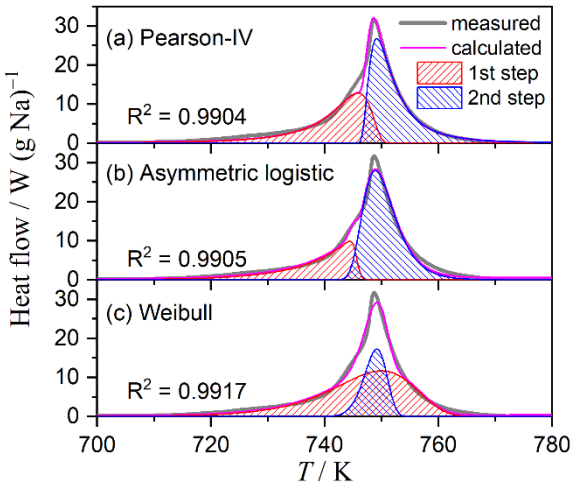

Figure S11. Typical results of the MDA using different statistical functions applied to the DSC curve for the liquid Na–$CaCO_3$ pellet reaction at a β of 5 K min^{-1}: (a) Pearson IV, (b) asymmetric logistic, and (c) Weibull functions.

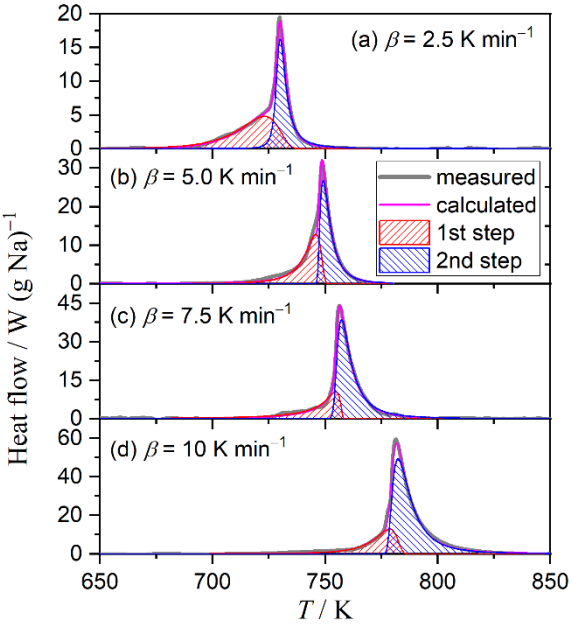

Figure S12. Results of the MDA using Pearson IV function for the liquid Na–$CaCO_3$ pellet reaction at different β values: (a) 2.5, (b) 5.0, (c) 7.5, and (d) 10 K min^{-1}.

The results of the MDA indicated systematic changes in the (c_1, c_2) values with β value: the decrease in the c_1 value and compensative increase in the c_2 value with an increase in the β value (Figure S13). The kinetic curves at different β values for each reaction step were obtained from the DSC peaks separated via MDA (Figure S14). The kinetic curves were subjected to the formal isoconversional analysis using the Friedman method, obtaining the $E_{a,i}$ values at different α_i values (Figure S15). Using the average $E_{a,i}$ value in the α_i range of 0.1–0.9, the experimental master plots

of ($d\alpha_i/d\theta_i$) versus α_i for each reaction step were obtained (Figure S16). Thereafter, the experimental master curves were fitted using the SB(m, n, p) function by optimizing the kinetic exponents (m_i, n_i, p_i) and A_i values. The kinetic parameters evaluated through MDA and the subsequent formal kinetic analysis are listed in Table S1, and they are used as the initial values for KDA.

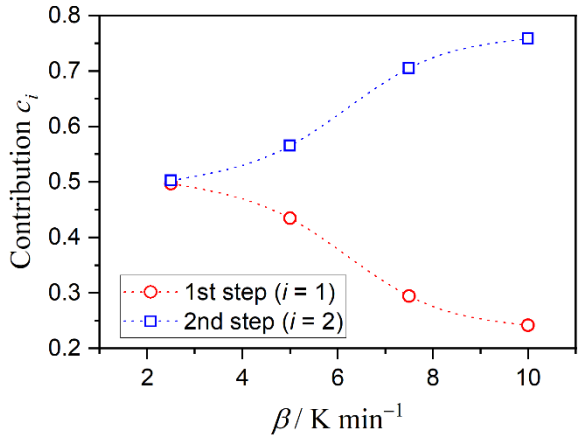

Figure S13. Changes in the contribution of each reaction step of the liquid Na–$CaCO_3$ pellet reaction with β determined via MDA.

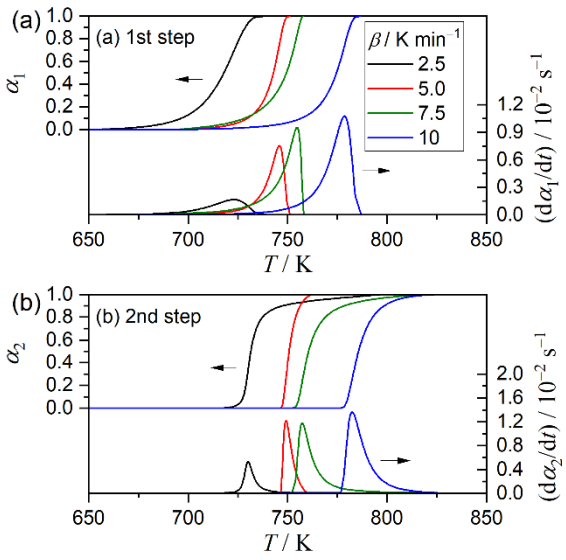

Figure S14. Kinetic curves for each reaction step of the liquid Na–$CaCO_3$ pellet reaction obtained via MDA: (a) first and (b) second reaction steps.

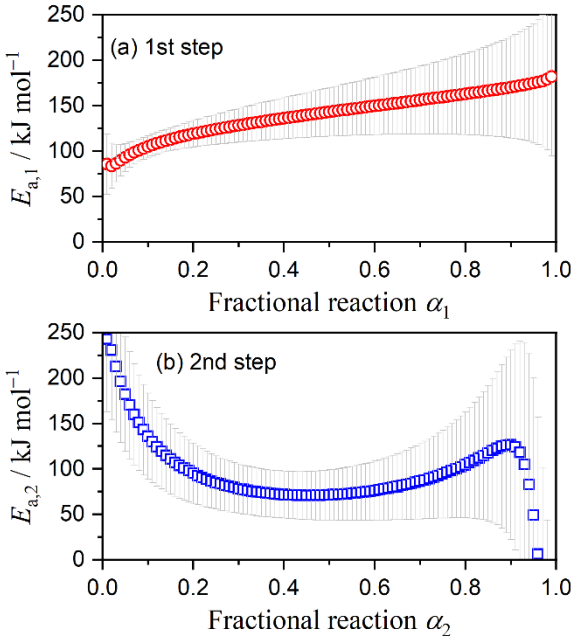

Figure S15. $E_{a,i}$ values at different α_i values for each reaction step of the liquid Na–$CaCO_3$ pellet reaction, calculated from the Friedman plot applied to the kinetic curves obtained via MDA: (a) first and (b) second reaction steps.

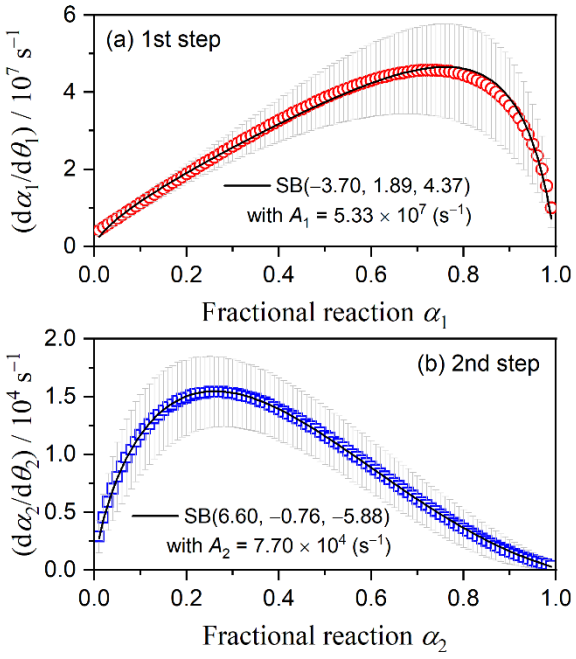

Figure S16. Experimental master plots of ($d\alpha_i/d\theta_i$) versus α_i for each reaction step of the liquid Na–$CaCO_3$ pellet reaction calculated from the kinetic curves obtained via MDA and using the average $E_{a,i}$ values: (a) first and (b) second reaction steps.

Table S1. Kinetic parameters for each reaction step of the liquid Na–$CaCO_3$ pellet reaction, determined through MDA and a subsequent formal kinetic analysis.

Kinetic parameter	First reaction step (i = 1)	Second reaction step (i = 2)
$E_{a,i}$ / kJ mol^{-1}, [a]	141.6 ± 17.7	89.1 ± 18.3
A_i / s^{-1}	(5.33 ± 0.15) × 10^7	(7.70 ± 0.64) × 10^4
m_i	−3.70 ± 0.31	6.60 ± 0.09
n_i	1.89 ± 0.12	−0.76 ± 0.04
p_i	4.37 ± 0.30	−5.88 ± 0.09
R^2, [b]	0.9941	0.9998

[a] Average over $0.1 \leq \alpha_i \leq 0.9$.
[b] Determination coefficient of the nonlinear least-squares analysis.